PAPER Submitted to the ITEA Conference, UTSI, Tullahoma, TN, October 12-15, 1999

MODEL INTEGRATED TESTING FOR DURABILITY ASSESSMENT OF TURBINE ENGINES

T.F. Tibbals[**], M. D. Sensmeier[**], and K. L. Nichol[*]
Sverdrup Technology, Inc., Arnold AFB, Tennessee
Al Stoner[***]
Pratt and Whitney, West Palm Beach, Florida
C. Biegl[****]
Vanderbilt University, Nashville, Tennessee

Abstract

Aeromechanical testing is conducted to define the vibratory characteristics of turbine engine structures for assessment of durability. These tests are typically conducted independent of the component design models, yet the pre-test strain/stress limit definitions have their origin in these models and subsequent component tests. Therefore the assumptions for the model become the assumptions for the engine test and subsequent data analysis. For instance, the mode identification is generally determined from the finite element method (FEM) model based upon frequency alone, *validated* via component bench testing, although changes in stress ratios based on engine to bench condition changes are not typically taken into account. To provide an assessment not only of the structural component but also of the design model, with the goal of correcting the design model for true engine operating conditions, the Structural Dynamic Response Analysis Capability (SDRAC) was developed at Arnold Engineering Development Center (AEDC). This capability processes strain gage (and eventually light probe displacement) data in near-real-time to assess the mode fit of the data to the FEM model simultaneously with the processing of the data against various failure criteria. This paper will describe the internal algorithms of SDRAC for determining the vibratory modes and establishing the fatigue integrity margin. An application of SDRAC on a recent test program will be discussed to demonstrate the concept and its utility for turbine engine aeromechanical assessment.

Background

Aeromechanical data is typically acquired by sweeping the engine RPM range for various operating conditions to excite the vibratory modes of the engine components. Classically, aeromechanical data processing and analysis has been performed by examining modes based upon frequency only, and utilizing scope limits and strain ratios on a per mode basis as a criterion for reliability. These scope limits were based upon a reduced-Goodman diagram to ensure a margin of safety was established. Strain ratios obtained from component lab testing or finite element analysis are used to identify the maximum stress level on installed components with minimal instrumentation (often a complete engine typically only has two straingages per blade). These strain ratios were obtained on a per mode basis. Peaks were sorted per mode and assembled into stress summaries to identify critical operating points. Low strain ratio data was typically ignored regardless of the stress value because of unreliability of extrapolating peak stress from such low strain ratios. Then these summaries were summarized further across many test periods to establish trends based upon transient parameters applicable to the operating environment (e.g., temperature, pressure, guide vane position, etc.). This classical aeromechanical evaluation process has been automated by the development of DatWizard at AEDC. This program utilizes the strain ratios and frequency bands for the different vibratory modes and generates the stress summaries automatically, immediately following the test point. A typical DatWizard analysis screen is shown in Figure 1, which shows a spreadsheet of the actual data, and a plot of peaks (stress in this case) on a modal basis.

[****] Research Professor

[***] Aeromechanical Structures Project Engineer

[**] Senior Engineer II

[*] Chief Engineer for Turbine Engine Structural Test & Evaluation

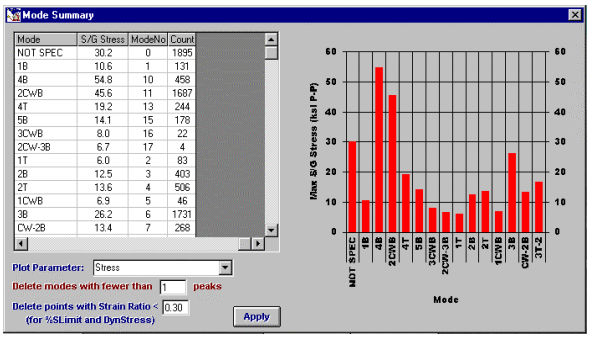

Figure 1. DatWizard Summary Analysis Screen

DatWizard also serves as the set-up interface to ensure a consistent setup amongst all of the data processing systems, as shown in Figure 4.

SDRAC Overview

The classical approach worked well for high aspect ratio blades, where the modes are widely spaced in frequency. However, with the advent of low aspect ratio blades and integrally bladed rotors (IBRs), the modes many times are too closely spaced to discern with frequencies only. Rather strain ratios across the blade must be used to properly identify the modes.

Peterson, et al1, first reported the concept for SDRAC in 1978. Development of the current capability began in 1988. Reference 2 describes the SDRAC in detail. As already stated, the SDRAC is essentially a tool that combines analytical models of a component with real time test data to assess the dynamic response characteristics for ***all locations*** on the component. A key element in the operation of the SDRAC is the finite element model. The model is used to define the geometry and to interpolate and extrapolate measured data to uninstrumented locations. Figure 2 illustrates the SDRAC analysis process.

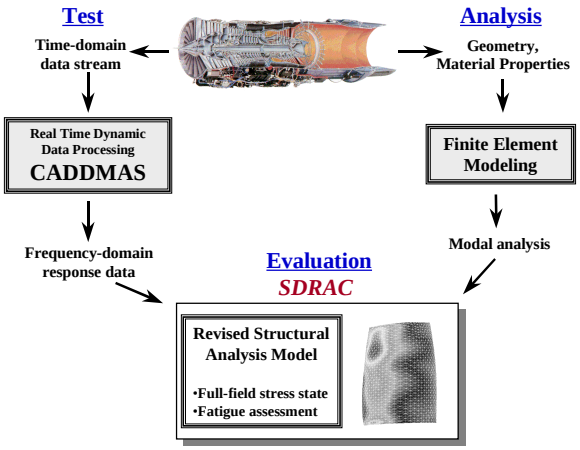

Figure 2. The SDRAC Analysis Process.

During the test, the SDRAC is fed a dynamic data stream from the AEDC developed Computer Assisted Dynamic Data Monitoring and Analysis System (CADDMAS)[3]. The CADDMAS converts the analog time-domain signal into frequency domain digital data in real-time using the fast Fourier transform (FFT) on a parallel-processing platform. This data is then used to discern which modes are responding and at what levels based upon frequency and strain ratios. Once responding modes are identified, the corresponding eigenvectors, $\vec{\phi}_i$, from the FEM model are selected and linearly summed according to the harmonic motion assumption to establish the overall response vector,

$$\bar{A}(t) = \sum_{modes} a_1\bar{\phi}_1 \sin(\lambda_1 t) + a_2\bar{\phi}_2 \sin(\lambda_2 t) + \ldots \qquad (1)$$

Figure 3 illustrates how this is done.

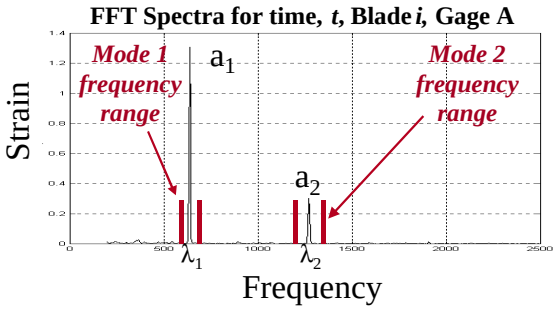

Figure 3. FFT mode selection.

This response is then compared with the straingages (minimum of two required per component) amplitudes and amplitude ratios to assess the validity of the model and its potential for predicting the complete component stress field. Modal stresses can be combined with the steady stresses in a stress-component consistent fashion for application to a given fatigue criteria. The Goodman fatigue criterion and some fracture mechanics tools are currently implemented.

A key feature of the SDRAC is the ability to accurately map "numerical" straingages to the finite element models for direct comparison with test strain data. These numerical straingages model the size of the straingage to account for averaging effects present in the test. This results in an "apples-to- apples" comparison of analytical and experimental strain values. The algorithms developed for this purpose are documented in [4].

The SDRAC can also be used in an off-line mode by reading CADDMAS stored time-domain files, CADDMAS stored Campbell diagram data files, and CADDMAS or Pre-Processor System (this system utilizes a CADDMAS front end only, no online monitoring displays) continuous frequency-domain peaks data files. The SDRAC has been used in both off-line and on-line modes for a number of recent engine programs, including the JSF program. The SDRAC can also be used on-line when no model of the component exists by using the strain ratios and scope limits in a classical aeromechanical analysis sense to monitor fatigue potential using the DatWizard setup files.

Finally, the AEDC aeromechanical analysis process using the two new tools is shown in Figure 4. What follows is a detailed description of the analytical techniques embodied in SDRAC.

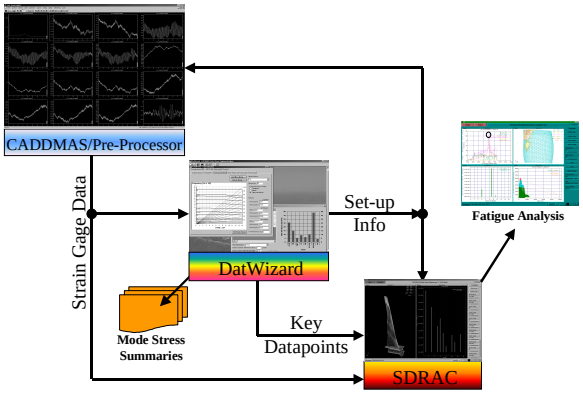

Figure 4. AEDC Aeromechanical Analysis Process

Mode Identification

Modal analysis is typically applied assuming the structure is in free vibration where the externally applied periodic loading is zero, and the vibration of the structure is primarily dependent upon the effects of the initial and boundary conditions only. Specifically, this process provides solutions of the problem

$$[M]\{\ddot{u}\}_i + [C]\{\dot{u}\}_i + [K]\{u\}_i = \{0\} \qquad (2)$$

Assuming $\{u\}_i = \{\phi\}_i Sin(\varpi_i t - \alpha_i)$ where $[M]$ is the mass matrix, $[K]$ is the stiffness matrix, $[C]$ is the damping matrix, $\{u\}_i$ is the i[th] mode nodal displacement vector, $\{\dot{u}\}_i$ is the i[th] mode velocity vector ($\dot{}$ implies time-derivative), $\{\ddot{u}\}_i$ is the i[th] mode acceleration vector, $\{\phi\}_i$ is the i[th] mode shape vector, ϖ_i is the i[th] mode radial frequency, α_i is the i[th] mode phase angle, and i is the mode index. For negligible damping, $[C] \cong [0]$, such that

$$[M]\{\ddot{u}\}_i + [K]\{u\}_i = \{0\} \qquad (3)$$

Substituting for $\{u\}_i$ yields

$$\left([K] - \varpi_i^2 [M]\right)\{\phi\}_i = \{0\} \qquad (4)$$

which is a set of N equations for N nodes of the model for each mode i of vibration. Equation (4) describes an eigenproblem, where the solutions $\{\phi\}_i$ are not unique in amplitude, but rather merely describe the relative motion of the nodes. A non-trivial solution (where the ϖ_i and the $\{\phi\}_i$ are not all zero) requires that

$$\det\left([K] - \varpi_i^2 [M]\right) = 0 \qquad (5)$$

which determines the natural radial frequencies, from which the mode shapes $\{\phi\}_i$ are obtained by substituting the ϖ_i back into the original homogeneous equation (4).

The above modal analysis approach assumes that the geometry is well defined to allow a suitable grid of finite elements (typically ten node tetrahedrons) to accurately describe the component displacements, and that the boundary conditions are known and adequately implemented. Centrifugal stiffening of the component is accounted for in the stiffness matrix $[K]$, resulting in the solutions $(\varpi_i, \{\phi\}_i)$ that are valid over some limited engine RPM range. To expand this range of validity, the SDRAC monitors the RPM and adjusts the steady stresses accordingly as a $f(\varpi_i^2)$.

Since SDRAC generates fatigue and stress monitoring displays based upon stress levels derived from FEM mode shapes, it is most critical that the modes of vibration be identified accurately. Consequently, the modes of vibration are identified by examining three distinct criteria. The first criterion is based strictly upon the peak vibration frequencies of the component obtained from FFT data. These peak frequencies are individually compared to the FEM models, and nodal displacement patterns for a given vibration frequency derived from component bench tests. A window is placed about these nominal analytical/experimental modal frequencies to account for centrifugal stiffening effects, temperature softening effects, and

changes in the boundary conditions. Figure 5 illustrates the modal frequency windows for a fan blade as a function of RPM. This plot is essentially a Campbell diagram, where the engine order lines crossing a natural frequency window indicates a potential for a critical operating region due to the potential for resonance.

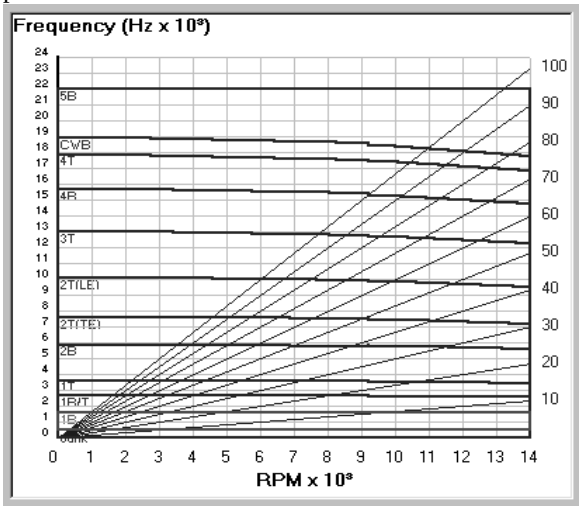

Figure 5. Frequency Windows on a Campbell Diagram.

Within SDRAC, the frequency fit is determined by maximizing

$$FFit_i = 1 - \left| 1 - \frac{f_i}{f_{0_i}} \right| = 1 - \frac{\sqrt{\left(f_{0_i} - f_i\right)^2}}{f_{0_i}} \qquad (6)$$

where f_i is the actual frequency and f_{0_i} is the nominal frequency for mode i, which may be determined from the FEM model or from component bench testing. Within SDRAC, f_{0_i} may be approximated as a function of RPM, if desired. This process returns a value in the interval $[0,1]$, where 1.0 is a perfect fit based upon frequencies alone. This term is called the frequency fit coefficient for mode i.

In regions where the frequency windows meet, or when multiple modes are excited simultaneously, additional criteria are necessary to discern the responding modes from which the component stresses will generated. Consequently, the second mode detection criterion is the ratio of strains from different positions on the blade. For a given mode shape, the ratio of the strains for each node with respect to a reference node (say the maximum) should be unique. Utilizing the component strain gages, the ratio of some number of gages at a given instant are compared with those from the FEM model for each mode near (i.e., within an input tolerance) the nominal frequency of oscillation to arrive at a coefficient describing the goodness of fit to the test mode. Let $\mathrm{E}_{FEM\,ij}$ be the FEM model strain for mode i at the location of gage j, and then $\vec{\mathrm{E}}_{FEM\,i} = \left\{\mathrm{E}_{FEM\,j}\right\}_i$ is the FEM model strain vector for all gages for mode i. Similarly, for measured strains, $\vec{\mathrm{E}}_{M\,i} = \left\{\mathrm{E}_{M\,j}\right\}_i$. Then the maximum least square mode amplitude may be described by

$$MA = \max\left(MA_i\right) = \max\left(\frac{\vec{\mathrm{E}}^T_{FEM\,i} \cdot \vec{\mathrm{E}}_{M\,i}}{\vec{\mathrm{E}}^T_{FEM_i} \cdot \vec{\mathrm{E}}_{FEM\,i}} \right) \qquad (7)$$

Now for each mode, an amplitude least squares mode fit coefficient may also be calculated as

$$AFit_i = \frac{MA_i}{MA} \qquad (8)$$

where $AFit_i = 1.0$ implies a perfect match to mode i based upon mode amplitude alone. The primary purpose for this parameter, however, is to steer the identification towards the large measured peaks. The other criteria described herein would otherwise settle on possibly some low amplitude noise peak if that happened to best fit the other criteria.

Finally, a third mode fit criterion is based upon the dot product of the actual mode vectors. Recall, for two vectors $\vec{a}$ and $\vec{b}$, the dot product

$$\vec{a} \cdot \vec{b} = \left|\vec{a}\right|\left|\vec{b}\right| Cos(\theta)$$

where θ is the angle between the two vectors. Therefore, the term $Cos(\theta) = \dfrac{\vec{a}^T \cdot \vec{b}}{\left|\vec{a}\right|\left|\vec{b}\right|}$ is a measure of the collinearity of the two vectors, i.e., $Cos(\theta) \to 1$ as $\theta \to 0$, implying the two vectors are collinear. Collinear reduced eigenvectors, one derived experimentally and the other derived from the FEM model, implies the nodal displacements for both must be the same, ***up to the uniqueness of these nodes describing the mode shape***. Since the component is typically not heavily instrumented, this uniqueness is not guaranteed. The mode fit coefficient is then calculated as

$$MFit_i = \frac{\vec{\mathrm{E}}^T_{FEM\,i} \cdot \vec{\mathrm{E}}_{M\,i}}{\left|\vec{\mathrm{E}}^T_{FEM\,i}\right|\left|\vec{\mathrm{E}}_{M\,i}\right|} \qquad (9)$$

Each of the three mode fit criteria can be combined utilizing weights appropriate for the confidence level one has in each of the criteria for a given situation, i.e.,

$$WFit_i = C_{mode} MFit_i + C_{amp} AFit_i + C_{freq} FFit_i$$

where C_{mode}, C_{amp}, and C_{freq} are the coefficients on the interval $[0,1]$ associated with the confidence in the mode fit, amplitude fit, and frequency fit criterion, respectively, for the component and vibration mode under investigation. Maximizing $WFit_i$ selects the i[th] mode, i.e.,

$$i \ni \max(WFit_i) = WFit_i$$

If each of these weights are set at 1/3, then each criterion is considered equally applicable. However, the effect of one fit coefficient could be minimized, such as C_{freq} if two modes were very close in frequency, such that the mode determination is heavily based upon the remaining two. In any case, the sum of the criterion weights must be equal to 1.0, i.e.,

$$C_{mode} + C_{amp} + C_{freq} = 1$$

Stress Evaluation

The stress field of a component is evaluated once the modes of vibration have been identified. In the FEM approach, the displacements determine the stresses/strains via the following considerations. First, the continuous displacement function for the element is based upon the nodal displacements derived from the eigenvectors via

$$\vec{u} = [N]\vec{\delta} = \sum_i^n \vec{\phi}_i \, Sin(\varpi_i t - \alpha_i) \qquad (10)$$

where $[N]$ is the shape function matrix for the element, n is the number of participating modes, and $\vec{\delta}$ is a vector containing the degrees of freedom for each node, i.e.,

$$\vec{\delta} = \{u_1 \; v_1 \; w_1 \; u_2 \; v_2 \; w_2 \ldots\}^T$$

where index j indicates node j, and u, v, and w are the local coordinates of the node.

With the displacements known across the element, the components of strain are calculated at each node of the FEM model by

$$[\varepsilon] = \frac{\partial \vec{u}}{\partial \vec{x}} = \frac{d[N]}{d\vec{x}}\vec{\delta} = [B]\vec{\delta}$$

These strains and the eigenvectors are then scaled to match the strains at the gage locations in a least squares sense. This is done by mapping the straingage onto the FEM model and suitably averaging the surrounding nodal strains to arrive at an equivalent strain for the center of the region occupied by the gage. Consider

$$\varepsilon_{Test_{\phi i}} = \begin{Bmatrix} a_i \\ b_i \end{Bmatrix} \qquad \varepsilon_{FEM_{\phi i}} = \begin{Bmatrix} j_i \\ k_i \end{Bmatrix}$$

$$\alpha_i = \frac{a_i j_i + b_i k_i}{a_i^2 + b_i^2}$$

then $\vec{\phi}_{i_{\text{Re sponse}}} = \alpha_i \vec{\phi}_{i_{FEM}} \qquad \sigma_{i_{\text{Re sponse}}} = \alpha_i \sigma_{i_{FEM}}$

Finally, the stress components at each node are calculated by

$$[\sigma] = [E][\varepsilon]$$

where $[E]$ is the elasticity matrix associated with the material of the component. For isotropic homogeneous materials, the stress equation is

$$\begin{Bmatrix} \sigma_{xx} \\ \sigma_{yy} \\ \sigma_{zz} \\ \tau_{xy} \\ \tau_{yz} \\ \tau_{zx} \end{Bmatrix} = \frac{E}{(1+\nu)(1-2\nu)} \begin{bmatrix} 1-\nu & \nu & \nu & 0 & 0 & 0 \\ \nu & 1-\nu & \nu & 0 & 0 & 0 \\ \nu & \nu & 1-\nu & 0 & 0 & 0 \\ 0 & 0 & 0 & \frac{1-2\nu}{2} & 0 & 0 \\ 0 & 0 & 0 & 0 & \frac{1-2\nu}{2} & 0 \\ 0 & 0 & 0 & 0 & 0 & \frac{1-2\nu}{2} \end{bmatrix} \begin{Bmatrix} \varepsilon_{xx} \\ \varepsilon_{yy} \\ \varepsilon_{zz} \\ \gamma_{xy} \\ \gamma_{yz} \\ \gamma_{zx} \end{Bmatrix}$$

where E is Young's modulus and ν is Poisson's ratio. Note that the uni-axial assumption is not made. Due to symmetry of the shear stresses, i.e., $\tau_{ij} = \tau_{ji}$, the stress components may be re-written as a stress tensor

$$\sigma = \begin{bmatrix} \sigma_{xx} & \tau_{xy} & \tau_{xz} \\ \tau_{yx} & \sigma_{yy} & \tau_{yz} \\ \tau_{zx} & \tau_{zy} & \sigma_{zz} \end{bmatrix}$$

The principal stresses can be calculated by diagonalization of the stress tensor, such that

$$\sigma_{Prin} = \begin{bmatrix} \sigma_1 & 0 & 0 \\ 0 & \sigma_2 & 0 \\ 0 & 0 & \sigma_3 \end{bmatrix}$$

where $\sigma_1 > \sigma_2 > \sigma_3$. The von Mises (distortional/octahedral) stress can be calculated from these nodal principal stress components via

$$\sigma_e = \frac{1}{\sqrt{2}}\left[(\sigma_2 - \sigma_1)^2 + (\sigma_3 - \sigma_1)^2 + (\sigma_3 - \sigma_2)^2\right]^{\frac{1}{2}}$$

The triaxiality factor, TF, is defined as the ratio of hydrostatic (first invariant or trace of stress tensor) to von Mises' stress:

$$TF = \frac{\sigma_1 + \sigma_2 + \sigma_3}{\frac{1}{\sqrt{2}}\left[(\sigma_1 - \sigma_2)^2 + (\sigma_2 - \sigma_3)^2 + (\sigma_3 - \sigma_1)^2\right]^{\frac{1}{2}}} = \frac{I_1}{\sigma_{eq}}$$

Calculating the triaxiality factor at each node allows for the plotting of triaxiality contours. In regions where $TF = 1.0$, a uniaxial condition exists. If $TF = 0.0$ a state of pure shear exists since the sum $\sigma_1 + \sigma_2 + \sigma_3$ (the first invariant of stress) is zero, which implies the stress state must be zero or no axial stresses exist. Finally, if $TF = 2.0$, then a biaxial state of stress exists in that region. Such contours serve to illustrate the fallacy of making the uniaxial assumption for critical regions of the component. Figure 6 shows the triaxiality contour for a twisted blade in first bending vibration.

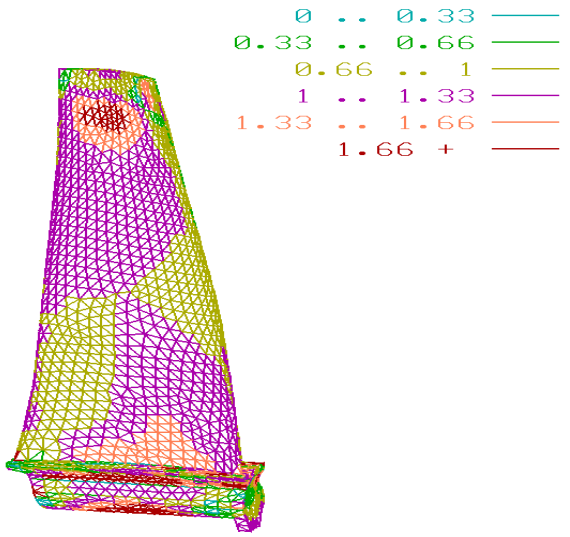

Figure 6. Twisted Blade Triaxiality Contour for First Bending Vibrational Mode.

Failure Criteria Comparisons

The Goodman diagram is the most basic fatigue failure criterion plotted. The Goodman diagram is plotted using von Mises stress to capture any non-uniaxial condition, however, for the node causing the peak stress, the maximum principal stress (σ_1) is also shown. Figure 7 shows a typical Goodman diagram showing the material limits for 100% and 60% levels.

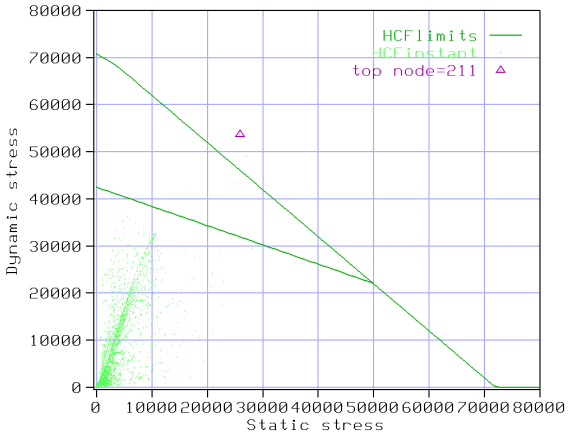

Figure 7. Goodman Diagram

Another fatigue monitoring approach is to plot blade contours of critical crack size based upon

$$a_{CR} = \frac{1}{\pi}\left(\frac{K_{TH}}{1.12 * K_t * \Delta\sigma_{\max}}\right)^2.$$

Here the threshold K value, K_{TH}, is for an input minimum crack growth rate (say 10^{-8} in/cycle), $\Delta\sigma_{\max}$ is the alternating stress observed (von Mises

stress is used, but the crack is assumed to be perpendicular to the max principal stress direction), and K_t is a stress concentration factor or a stress margin factor. For the worst blade location (region), an arrow-aligned perpendicular to the σ_1 direction indicates its theoretical propagation relative to the edge of the blade.

Still another approach is to use the MIL-HNBK-5G or similar crack growth curve, and then for an input crack interval [a1, a2], integrate the area under the inverse of the curve for the range of the [a1, a2] to find the expected life of the component in cycles. This would be performed for a closed-form solution for the crack growth curve, probably based upon the Paris Law (which fits the center linear portion of the curve)

$$\frac{da}{dN} = C * \Delta K^m = C * \left(1.12 * K_t * \Delta\sigma * \sqrt{\pi * a}\right)^m$$

.

This would be calculated for each node such that a blade life contour could be generated. In addition, the minimum life and its node should be specified in a box somewhere, which I guess could be updating in real-time. Infinite life would be assumed to be 10^9 cycles, and this would be the green contour, with the lowest life being red. Alternatively, one could input just the minimum detectable crack size, and then the critical crack length could be calculated from $K_{\max}$ given $\sigma_{Alternating_{\max}}$ and used for a2.

A final approach is to use a given input minimum detectable crack size, a_{md}, along with the peak stresses and plot this for all nodes on the $\frac{da}{dN}$ vs ΔK curve, where the alternating stress is used to determine ΔK

$$\Delta K = 1.12 * K_t * \Delta\sigma * \sqrt{\pi * a_{md}} .$$

In this case one hopes to stay near the threshold or at least in the lower linear region of the crack propagation curve. SDRAC can also plot $\frac{da}{dN}$ contours on the component model.

Strain Energy Density (SED)

"Failure of material elements in a solid is caused by permanent deformation or fracture which can be related to shape change (distortion) and volume change (dilatation)" [ref. Gdoutos, 1990]. The strain energy density criterion of failure is based upon the energy storage capacity of a differential volume of material. Consequently, this criterion is yield based, which is similar to the von Mises' Maximum Distortional Energy (Octahedral Shear Stress Energy) criterion. However, SED includes the dilatational component in addition to the von Mises' distortional component, and can predict the onset of failure via yielding or fracture in ductile materials. The pertinent SED equations are:

$$SED = \frac{dW}{dV} = \left(\frac{dW}{dV}\right)_{distortion} + \left(\frac{dW}{dV}\right)_{\Delta volume}$$

$$\left(\frac{dW}{dV}\right)_{distortion} = \frac{(1+\upsilon)}{3E}\sigma_{eq}$$

$$\left(\frac{dW}{dV}\right)_{\Delta volume} = \frac{(1-2\upsilon)}{6E}\left(\sigma_x + \sigma_y + \sigma_z\right)^2$$

$$SED = \frac{(1+\upsilon)(1-2\upsilon)}{6E}\left[\left(\sigma_x + \sigma_y + \sigma_z\right)^2 + 2\sigma_{eq}^2\right]$$

A contour of SED doesn't directly provide much more information than a simple von Mises' stress plot. However, the interpretation of the SED component ratios provides a measure of the potential for failure and the mode of failure (yielding or fracture). Let

$$R_{SED} = \frac{\left(\frac{dW}{dV}\right)_{\Delta volume}}{\left(\frac{dW}{dV}\right)_{distortion}} = \frac{(1-2\upsilon)}{2(1+\upsilon)}\frac{\left(\sigma_x + \sigma_y + \sigma_z\right)^2}{\sigma_{eq}^2}$$

,

if $R_{SED} > 1.0$, then fracture failure is predicted at the location of $SED_{\min}$, while if $R_{SED} < 1.0$, then yielding failure is predicted at the location of $SED_{\max}$. Contour plots of fracture potential and of yield potential are included in SDRAC.

Socie Parameter

The Socie Parameter [ref. Langlais, et al, ASTM STP 1303, 1997] provides an indication of the potential for failure due to stresses on a critical shear plane. The Socie model is based upon shear and is defined as

$$\gamma_{\max}\left(1 + \eta\frac{\sigma_{\gamma_{\max}}}{\sigma_{Yield}}\right) = \frac{\tau'_f}{G}\left(2N_{fS}\right)^b + \gamma'_f\left(2N_{fS}\right)^c ,$$

where N_{fS} is the fatigue life for pure shear, and the primed components are the shear fatigue ductility factors. The Socie Parameter, SP, is the LHS of this multi-axial fatigue model. This parameter does for shear what the Smith-Watson-Topper parameter does for tension

$$\sigma_{\max}\varepsilon_a = \frac{\sigma_f'^2}{E}\left(2N_{fT}\right)^b + \frac{\eta}{2}\left(1+\upsilon_e\right)\sigma_f'\varepsilon_f'\left(2N_{fT}\right)^c$$

,

where N_{fT} is the fatigue life for pure tension, and the primed components are the tensile fatigue strength factors. Both of these models are extensions of the Basquin equation for accounting for mean stress effects in uniaxial data. The following steps are used to determine the Socie Parameter:

1. Determine the principal strains from eigenvalues:

$$\varepsilon = \begin{bmatrix} \varepsilon_{xx} & \gamma'_{xy} & \gamma'_{xz} \\ & \varepsilon_{yy} & \gamma'_{yz} \\ Symm & & \varepsilon_{zz} \end{bmatrix} \qquad \det\left(\varepsilon - \lambda I\right) = 0,$$

where $\gamma'_{ij} = \frac{1}{2}\gamma_{ij}, \quad i \neq j, \quad \lambda_{\max} = \varepsilon_1$

2. Find eigenvector (direction cosines) $\varepsilon\vec{V}_i$, then $\theta_{\gamma_{\max}} = Cos^{-1}\left(\varepsilon\vec{V}_{i1}\right) + \frac{\pi}{4}$ defines the maximum shear plane with respect to the principal normals, $\varepsilon\vec{V}_{11}$ being the first (maximum) term of $\varepsilon\vec{V}_1$ the maximum eigenvector, then $\gamma_{\max} = \left|\lambda_{\max} - \lambda_{\min}\right|$.

3. The maximum normal stress associated with this maximum shear strain is $\sigma_{\gamma_{\max}} = \varepsilon\vec{V}_1\sigma\,\varepsilon\vec{V}_1$ where $\sigma = \begin{bmatrix} \sigma_{xx} & \tau_{xy} & \tau_{xz} \\ & \sigma_{yy} & \tau_{yz} \\ Symm & & \sigma_{zz} \end{bmatrix}$. This is the equivalent crack opening tensile stress, assuming the crack propagates on the plane of maximum shear.

4. Finally, $SP = \gamma_{\max}\left(1 + \eta\frac{\sigma_{\gamma_{\max}}}{\sigma_{Yield}}\right)$, where η is an input, typically $\eta = 0.5$.

For multi-axial fatigue, a conservative estimate of the life, N, may be determined by

$$\frac{1}{N} = \frac{1}{N_{fT}} + \frac{1}{N_{fS}},$$

and contours of this life are plotted within SDRAC.

Application

For this test program, DatWizard was used to identify key data points, where SDRAC was to be applied. SDRAC was then run for these data points. SDRAC's spectra plots confirmed the participating modes. At this point, to minimize algebraic contribution of inactive modes, which may be noisy, bad straingage channels and poor fitting modes may be turned off. This essentially acts as a filter, since most data has a broadband response below some threshold. Consequently, this ensures that false readings are not obtained due to high stress modes being excited by noise during the harmonic summation. Figure 8 shows a %-Goodman time-history plot for the data point.

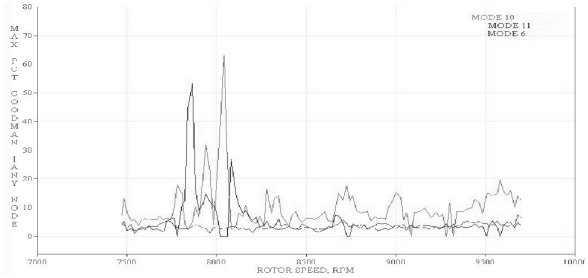

Figure 8. SDRAC %-Goodman Time-History

These traces are the maxima for the three selected modes, 6 (benign), 10 (4th LE Bending), and 11 (2nd Chordwise Bending), obtained from the FEM model, for ***anywhere*** on the component. Each point of each trace is determined by searching the whole component for the maximum stress for the selected mode, and then computing %-Goodman limit based upon input Goodman data and criterion. This plot can be built in near real-time, such that this plot immediately indicates critical rotor speeds and the potential for fatigue. Since this plot is for only the selected modes, it is much more explicit than a heavily blackened Campbell diagram when several modes are excited at once (as in a bladed disk configuration). As shown in Figure 9, the Goodman

diagrams can also be plotted directly utilizing the same sorted points, however, the RPM at which the critical stress occurred is no longer available.

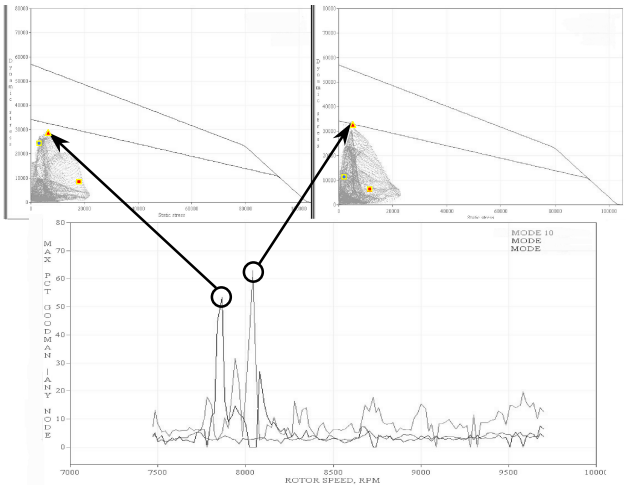

Figure 9. Goodman Diagrams Corresponding to the %-Goodman Time-History

Note that in Figure 9 the straingage maxima are also located (square enclosed 'x' data points) on the Goodman-Diagram. For this test, note that the straingage maxima are much lower for the 2CWB mode (right Goodman) than the peak identified by SDRAC.

Finally, the component may be animated to illustrate the vibrational mode, as shown in Figure 10. The straingage parameters and their locations are shown on the component. Obviously, these animations are exaggerated for visualization purposes, but they do demonstrate the mode (or modes) and the stress field fluctuations due to the mode (or modes). In addition, the visualization can show the effect of harmonic summation on the distortion of the pure modes, as well as, illustrate the susceptibility of the gages to respond to the given mode.

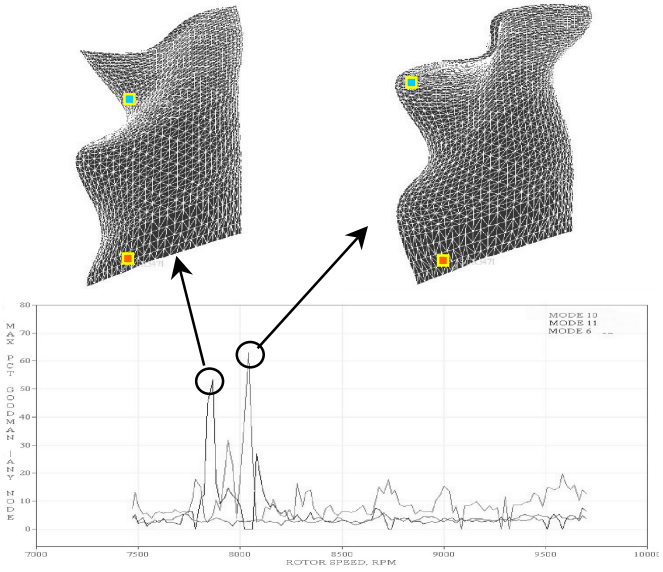

Figure 10. Blade Deformation animation for the %-Goodman Time-History

For this particular test, it can be seen in Figures 11and 12 that two different parameters can give two different %-Goodman and stress values for the **same component maximums** based upon mode identification via frequencies and strain ratios alone.

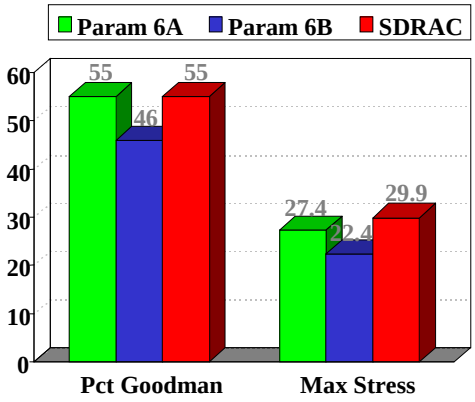

Figure 11. Parameter and SDRAC comparisons for 4th Bending

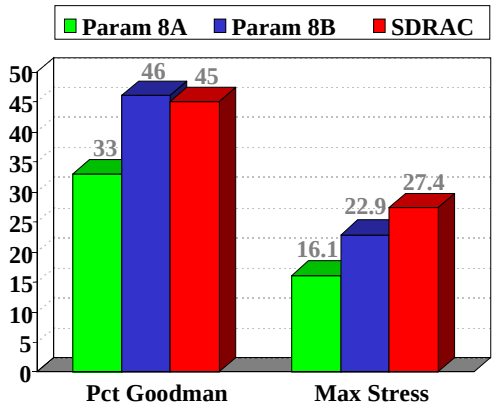

Figure 12. Parameter and SDRAC comparisons for 2nd Chordwise Bending

The more sophisticated mode identification criterion in SDRAC resolved the inconsistencies of these two parameters, and provided a single value for the maxima. In addition, SDRAC correctly distinguished the critical mode for this test as the 2nd chordwise bending mode instead of the 4th LE Bending mode as shown from DatWizard in Figure 1. Finally, SDRAC showed that the peaks stresses were slightly higher than that indicated by the classical technique (possibly due to multi-mode interaction). In this sense, SDRAC complements the classical aeromechanical analysis approaches, and can act as an arbitrator for inconsistencies.

Summary

Development programs for new engine systems are generating significantly greater volumes of dynamic data than ever before. New engine systems are also seeking to extract greater and greater work from each stage of the machine. These factors highlight a need to increase understanding of the structural integrity of each component and to bring understanding to all of the data generated. The SDRAC has been developed to meet these challenges. As shown, the SDRAC combines the strengths of state-of-the-art dynamic data processing technology and finite element modeling technology to produce a single tool that permits real time analysis of the modal characteristics of an engine component and performs fatigue analysis to insure that newly developed components meet their structural integrity goals. The SDRAC has been used successfully on a variety of test programs, and has demonstrated its advantages over the classical aeromechanical approaches.

References

1. Peterson, M.R., Alderson, R.G., Stocton R.J. Tree, D.J., “Three-Dimensional Finite-Element Techniques for Gas Turbine Blade Life Prediction”, AGARD-CP-248, pp. 9-1 – 9-14, 1978.
2. Nichol, K.L., M. D. Sensmeier, M.D., Tibbals, T.F., “Assessment of Turbine Engine Structural Integrity using the Structural Dynamic Response Analysis Code (SDRAC)”, IGTI-99-095, ASME Turbo Expo ‘99, Indianapolis, IN, June 6-10, 1999.
3. Tibbals, T.F., Bapty, T.A., Abbott, B.A., “CADDMAS: A Real Time Parallel System for Dynamic Data Analysis”, ASME Paper No. 94-GT-194, June 1994.
4. Nichol, K.L., “Numerical Strain Gage Representation”, Proceedings of the 39th AIAA/ASME/ASCE /AHS/ASC Structures, Structural Dynamics and Materials Conference, Long Beach, CA (to be published), April 1998.